Computers, Environment and Urban Systems 96 (2022) 101847

Contents lists available at ScienceDirect

Computers, Environment and Urban Systems

journal homepage: www.elsevier.com/locate/ceus

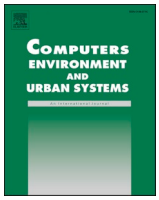

Exploring the effect of urban spatial development pattern on carbon dioxide emissions in China: A socioeconomic density distribution approach based on remotely sensed nighttime light data

Shirao Liu [a,b,1], Jingwei Shen [a,b,1], Guifen Liu [c], Yizhen Wu [a,b], Kaifang Shi [a,b,*]

[a] Chongqing Jinfo Mountain Karst Ecosystem National Observation and Research Station, School of Geographical Sciences, Southwest University, Chongqing 400715, China
[b] Chongqing Engineering Research Center for Remote Sensing Big Data Application, School of Geographical Sciences, Southwest University, Chongqing 400715, China
[c] Shandong Provincial Eco-environment Monitoring Center, Jinan 250000, China,

ARTICLE INFO

Keywords:
Urban spatial development pattern
Carbon dioxide emissions
Nighttime light data
NPP-VIIRS
Socioeconomic density distribution
China

ABSTRACT

Exploring *the effect of urban spatial development pattern* (UPD) *on carbon dioxide emissions* (CDEs) (EUC) is important for understanding low-carbon sustainable development. Numerous studies on EUC have mainly focused on individual cities or regions within the mixed conclusions due to the lack of reliable UPD indices and reasonable methods. Thus, taking China's 257 prefecture-level cities as experimental objects, a novel system approach was developed from the perspective of *socioeconomic density distribution* (SED) index to measure UPD on the basis of *the Suomi National Polar-orbiting Partnership* (NPP) *visible infrared imaging radiometer suite* (VIIRS) nighttime light data. EUC was then analyzed on the basis of the dynamic panel data model from multiple perspectives. Results show that the SED index can effectively measure UPD with rich spatial information from multiple dimensions. The coefficients of SED and $(SED)^2$ are 0.129 and − 1.240, respectively, indicating that EUC shows a clear inverted U-shaped curve in China, i.e., an increase in UPD compactness increases CDEs at the beginning, and when a certain height is reached, an increase in UPD compactness decreases CDEs. Heterogeneity analysis indicates a U-shaped curve of EUC is found in megalopolis, and inverse U-shaped curve are observed in medium and small cities. Bus passenger volume, energy consumption, infrastructure, and housing demand are proven as the transmission factors of EUC. It is suggested that utilizing the positive externality effect of agglomeration and accelerating the inflection point of the inverse U-shaped curve may be necessary because the improvement of urban socioeconomic agglomeration will improve the UPD compactness and reduce CDEs.

1. Introduction

The rapid urbanization progress in China has led to a sustained growth in *carbon dioxide emissions* (CDEs) related to energy consumption since the reform and opening up (Sun, Han, & Li, 2020). Faced with the continuous growth of CDEs, the Chinese government pledged at the 21st United Nations Climate Change Conference in 2015 to lower CDEs intensity by 60%—65% by 2030 compared to 2005 levels (Wang & Huang, 2019). At the General Debate of the 75th Session of the United Nations General Assembly in 2020, the Chinese government further stated explicitly that CDEs will peak by 2030 and strive to achieve carbon neutrality by 2060. Therefore, how to achieve the CDEs reduction target has become the current focus of Chinese society.

Many scholars and policy makers have realized energy conservation and emission reduction through advocating public transportation, optimizing industrial structure, promoting technological progress, and developing low-carbon economy (Shi, Shen, Wu, et al., 2021; Wang, Wang, Fang, et al., 2019a), and *the urban spatial development pattern* (UPD) has also been considered to affect the generation and diffusion of CDEs to a great extent (Sun et al., 2020). UPD involves the spatial evolution and replacement process of the "dispersion-compactness" of various socioeconomic elements, including economic activities,

* Corresponding author at: Chongqing Jinfo Mountain Karst Ecosystem National Observation and Research Station, School of Geographical Sciences, Southwest University, Chongqing 400715, China.
E-mail addresses: msnlsr@email.swu.edu.cn (S. Liu), sjwgis@swu.edu.cn (J. Shen), jnhbjliuguifen@jn.shandong.cn (G. Liu), wyz19981013@email.swu.edu.cn (Y. Wu), skffyy@swu.edu (K. Shi).
[1] Co-first author of this work.

https://doi.org/10.1016/j.compenvurbsys.2022.101847
Received 17 December 2021; Received in revised form 5 June 2022; Accepted 8 June 2022
Available online 14 June 2022

population, urban land, and other public facilities (Liang, Liu, & Li, 2021). Theoretically, the more compact the UPD, the higher the *socio-economic density distribution* (SED). On the contrary, the more dispersed the UPD, the lower the SEDs (Fig. 1). The lock-in effect of UPD is significant in changing urban energy consumption and CDEs level (Kahn, 2009). For example, a compact UPD can shorten people's commuting distance and time, making them more inclined to use public transportation and then reducing CDEs (Liang et al., 2021). By contrast, a compact UPD can cause traffic congestion, which is unconducive to lower CDEs (Wang & Huang, 2019). A dispersed UPD can increase consumption, waste of energies, and CDEs (Sun et al., 2020), which is conducive to reducing urban road density and possibly reducing CDEs by reducing people's desire to travel. Thus, *the effect of UPD on CDEs* (EUC) is theoretically decided by the relative magnitude of the above effects.

Effective quantification of UPD is an important prerequisite for exploring EUC. Many indicators, including landscape pattern index (Shi, Wang, Yang, et al., 2019), land use intensity (Mubarek, Koomen, Estreguil, et al., 2011), population density (Liang et al., 2021) and economic density (Henderson, Nigmatulina, & S. K., 2019), are used to represent UPD. No vertical socioeconomic information is found because landscape pattern index and land use intensity only reflect the changes in urban physical structure, thereby limiting their wide applications. Population density and economic density can accurately reflect the regional urban structure because they can represent regional economic development and spatial agglomeration (Henderson et al., 2019; Liang et al., 2021). Specifically, population density and economic density can represent the expansion and contraction of the ranges of population and economy development in the horizontal direction and the intensity of population and economy activities in the vertical direction (Fig. 2). Although the two indicators have been applied extensively in studies of environmental pollution impacts of urban development, the existing studies are limited by the following three aspects. First, population density or economic density can only reflect one-dimensional (1D) aspect of population or economy, and UPD is a multidimensional system in nature, which involves all aspects of socioeconomic elements. Second, population density or economic density cannot effectively identify spatial UPD owing to the shortage of spatial information (Ciccone & R. H., 1996; Zhao, Cao, & Ma, 2020). Statistics are widely used to calculate population density or economic density, but the data can only reflect the average density at administrative scales, failing to reflect the differences in the distributions of population density or economic density within a city (Henderson et al., 2019; Liang et al., 2021). Third, existing studies often focused on a certain region or a time period and lacked of large-scale and long time-series analysis due to the data limitations.

With the development of remotely sensed technology, *remotely sensed nighttime light data* (NTL) provide an excellent means to measure *gross domestic product* (GDP), population, urbanization level, and other socioeconomic indicators (Liu, Shi, Wu, et al., 2021; Shi, Huang, Yu, et al., 2014; Shi, Yu, Huang, et al., 2014). Liu et al. (Liu et al., 2021) summarized that the NTL can characterize socioeconomic development in four dimensions: demographic, economic, social, and spatial aspects. Thus, the NTL can provide rich SED information from multiple dimensions to compensate for the 1D and no spatial information deficiencies on the UPD quantification. Currently, the NTL are primarily derived by *the Defense Meteorological Satellite Program-Operational Line-scan System* (DMSP-OLS) data and *the Suomi National Polar-orbiting Partnership-visible infrared imaging radiometer suite* (NPP-VIIRS) data (Shi, Huang, et al., 2014; Shi, Yu, et al., 2014). Compared with DMSP-OLS data with a spatial resolution of 1000 m, which are updated only to 2013, the NPP-VIIRS data are still being updated with better radiometric and spatial resolutions without pixel saturation (Tang & Cui, 2017). Many studies demonstrated that NPP-VIIRS data outperform DMSP-OLS data in the estimation of socio-economic indicators; thus, they are usually preferred in urban applications (Shi et al., 2021).

Based on time-series NTL, the aim of this study is to investigate China's EUC from a SED approach. To achieve the above objective, taking China's 257 prefecture-level cities as experimental objects, we first developed a SED index to characterize UPD based on the NTL. We then used this index to explore EUC on the basis of the dynamic panel data model from multiple perspectives. This study addresses the following questions: (1) How can UPD be identified effectively from a SED approach based on the NTL? (2) What is EUC in China?

2. Literature review

An accurate identification of UPD is the premise for investigating EUC. Some studies have identified UPD on the basis of statistics. Zhao et al. (Zhao, Cao, & Ma, 2020) chose a location entropy as the indicator to measure industrial agglomerations by using statistics on 30 provincial

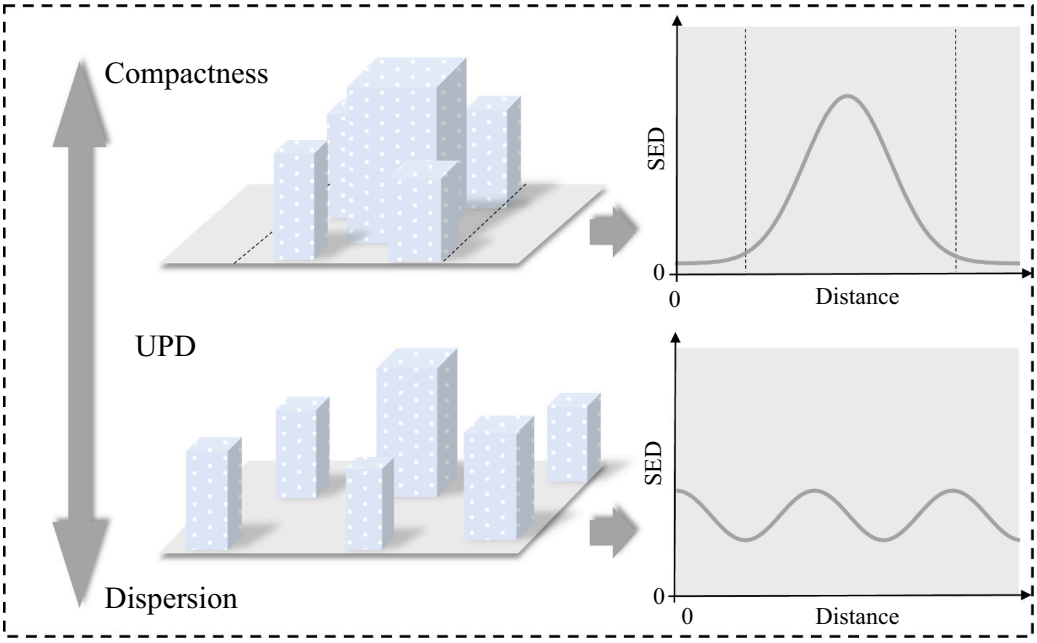

Fig. 1. SEDs within different UPDs.

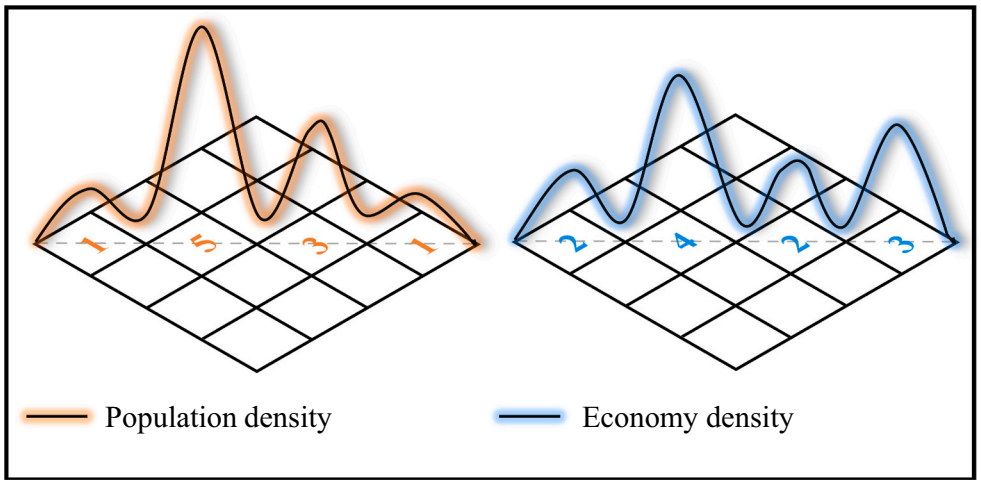

Fig. 2. Horizontal and vertical distributions of population density and economic density.

administrative regions in China. Ciccone and Hall (Ciccone & R. H., 1996) calculated the density of economic activity on the basis of statistics on 50 states in America. Some studies have utilized spatial data, such as LandScan population data, to assess UPD (Hankey & Marshall, 2010; Henderson et al., 2019; Liang et al., 2021). Henderson et al. (Henderson et al., 2019) used different economic density approaches to measure the pull force of cities on the basis of LandScan population data. Liang et al. (Liang et al., 2021) used LandScan population data to identify UPD from the perspective of population density distribution on prefecture-level cities in China. Hankey and Marshall (Hankey & Marshall, 2010) measured UPD by using linear population density on 142 cities in America. Other studies have used optical remote sensing images, such as Landsat satellite images or land cover data, to identify urban spatial structures. Mubarek et al. (Mubarek et al., 2011) constructed a composite index by using four indices for representing UPD's compactness on the basis of Landsat satellite images on 'large urban zones' in Europe. Shi et al. (Shi, Wang, et al., 2019) calculated landscape pattern indices to characterize UPD on the basis of land cover data in China. Studies on the UPD cannot effectively reflect the differences in SED distributions within a city owing to the shortage of spatial information. 1D LandScan population data cannot comprehensively reflect multidimensional UPD involving economic activities, population, mixed development of land, and other aspects (Liang et al., 2021). UPDs related to Landsat satellite images or land cover data can only represent the changes in urban physical structure but not the longitudinal socioeconomic information.

Numerous studies have confirmed that NTL are closely correlated with socioeconomic indicators, such as population, economy, and urban land (Liu et al., 2021; Shi, Huang, et al., 2014; Shi, Yu, et al., 2014), which can compensate for 1D and no spatial defects. From the horizontal dimension, NTL can effectively identify urban spatial development scope (Shi, Huang, et al., 2014). From the vertical dimension, NTL can accurately represent the spatial distribution differences in socioeconomic activities within a city (Shi et al., 2021; Shi, Yu, et al., 2014).

Currently, the environmental performance of UPD, especially the effect on CDEs, has received less attentions. Available studies on UPD's impacts mainly focused on the relationship between SED agglomerations and environmental pollutions, and the conclusions can be divided into the following three categories roughly.

- A one-way linear relationship is found between SED agglomerations and environmental pollutions. One view holds that agglomerations can present positive externalities by promoting enterprise cooperation and improving production efficiency, so as to reduce environmental pollutions. Zhao et al. (Zhao, Dong, & Dong, 2021) believed that producer services' agglomerations can reduce pollutions. Zhao et al. (Zhao, Cao, & Ma, 2020) pointed out that industrial agglomerations will be conducive to improving environmental quality. Another view is that agglomerations will increase environmental pollutions. Dong et al. (Dong, Wang, Zheng, et al., 2019) concluded that industrial agglomerations can aggravate environmental pollutions in China at the national and provincial levels. Cheng et al. (Cheng, 2016) investigated the relationship between manufacturing agglomerations and environmental pollutions and indicated that manufacturing agglomerations can aggravate environmental pollutions.
- The relationship between SED agglomerations and environmental pollutions presents a nonlinear trend. Guo et al. (Guo, Tong, & Mei, 2020) concluded that the relationship between industrial agglomerations and green development efficiency presents a U-shaped curve in Northeast China. Wang and Wang (Wang & Wang, 2019) analyzed how industrial agglomerations affects the environmental performance at prefecture-level cities and found a U-shaped curve between industrial agglomerations and environmental performance. Chen et al. (Chen, Sun, Lan, et al., 2020) examined the contribution of industrial and service industry agglomerations on environmental pollutions at prefecture-level cities and concluded that agglomerations are significantly related to wastewater emissions, sulfur dioxide emissions, and soot emissions in an inverse U-shaped curve relationship.
- An interactive relationship is found between SED agglomerations and environmental pollutions. Cheng et al. (Chen et al., 2020) found that manufacturing agglomerations and environmental pollutions have two-way effects by taking China's prefecture-level cities as the basic research units. Manufacturing agglomerations can aggravate environmental pollutions, while environmental pollutions restrained manufacturing agglomerations.

Studies have also examined the relationship between urban form and CDEs by expanding on the relationship between SEDs and environmental pollution. For example, Makido et al. (Makido, Dhakal, & Yamagata, 2012) concluded that there is an inverse relationship between the compactness of urban form and CDEs by examining the relationship between urban form and CDEs from urban areas in 50 cities in Japan, i.e. the higher the compactness, the lower the urban carbon emissions. Wang et al. (Wang, Wang, Fang, et al., 2019b) argued that increased irregularity in urban form reduces the efficiency of CDEs. In contrast, the compactness of urban areas is considered to have a significant positive effect on CDEs efficiency. Yang et al. (Yang, Li, & Cao, 2015) described urban form in terms of urban population density and

average city size and concluded that urban population density and average city size have a significant positive effect on transport CDEs per capita. We summarized three deficiencies by reviewing these relationships. First, controversial results remain in existing studies. Three relationships, namely, a one-way linear relationship, a nonlinear relationship, and an interactive relationship, are observed. These mixed results cannot provide scientific references for the sustainable development of urban socioeconomic environment. Second, unreliable UPD quantification approach and rough estimation regressions are widely used in previous studies. Traditional UPD method cannot effectively identify urban spatial development from the horizontal and vertical dimensions. The widely used linear regression method and the lack of robustness test lead to the bias of the results. Third, the heterogeneity and mechanism of EUC have been assessed quantitatively to a limited extent in existing studies, but these types of analyses are of great importance for understanding the urban environmental sustainability.

3. Study area and data sources

3.1. Study area

Prefecture-level cities in mainland China (including four major municipalities) were selected as the basic experimental units. Prefecture-level cities were taken as research samples for the following reasons. First, the administrative unit within prefecture-level cities, including municipal district, county, and county-level city, are closer geographically and have similar political, economic, cultural, and natural geographical environment (Chien, 2010). Prefecture-level cities are theoretically regraded as research units, which are closely connected internally and relatively independent externally (Wang & Wang, 2019). This condition is because the independence of each administrative region makes external economic barriers formed between cities. Second, provincial administrative regions cannot manage county-level administrative regions directly across prefecture-level cities. Prefecture-level cities, as a "bridge" connecting the two, can connect provincial policies and measures directly and plan and coordinate the development of county-level units (Chien, 2010). Finally, considering that the inconsistency of the research spatial scale, the research conclusions may not be widely applicable. Few empirical analyses of EUC are reported at the prefecture-city scale. Thus, taking prefecture-level cities as research unit can enrich the research results at this unit scale. The administrative districts were merged and unified on the basis of 2018, and 257 prefecture-level cities were ultimately selected as study samples after eliminating the cities with missing values and outliers. For subsequent heterogeneity analysis, the sample cities were divided into four sizes (Fig. 3).

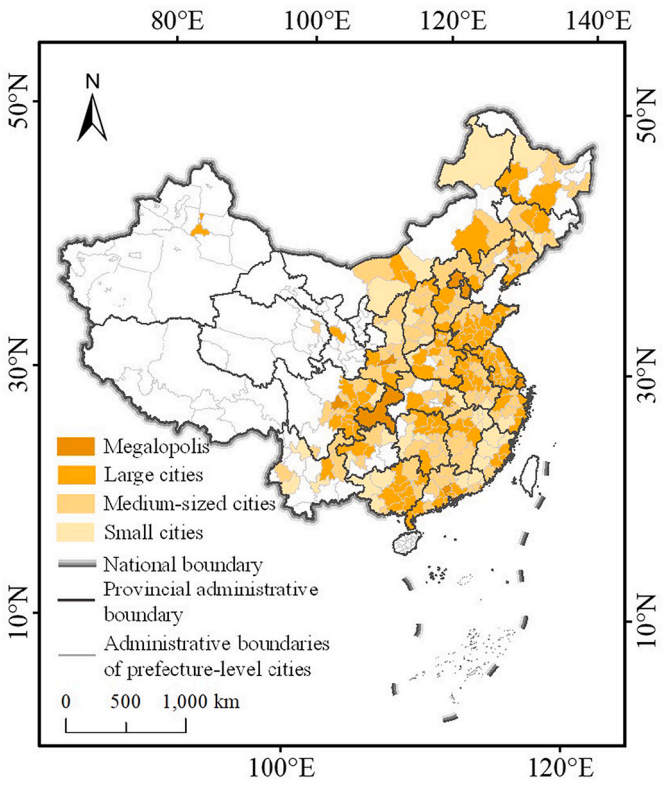

Fig. 3. Spatial distributions of the selected prefecture-level cities. Note: selected prefecture-level cities are divided into megalopolis (>5 million), large cities (1–5 million), medium-sized cities (0.5–1 million), and small cities (<500,000) on the basis of the number of registered population at the end of 2018 in accordance (State Council, 2014).

3.2. Data sources

Five types of data, namely, monthly NPP-VIIRS data, CDEs data, socioeconomic data, land cover/use data, and administrative boundaries, were collected. Descriptive information on data sources is listed in Table S1. All spatial data projected onto the WGS84-Albers projection, and resampled to a spatial resolution of 500 m.

Monthly NPP-VIIRS data are generated from the Earth Observations Group at NOAA's National Centers for Environmental Information. Since April 2012, the version 1 VIIRS composites are obtainable every month. The monthly NPP-VIIRS products consist of two profiles. The first one, "vcmcfg", does not include data affected by stray lights; the second one, "vcmslcfg", has a wider coverage for two poles, but is of poorer quality because it includes stray lights (Yang, Wu, Wang, et al., 2021). The "vcmcfg" was made use of to ensure data quality in this study. In addition, auroras, fires, and other transient light sources are still contained in the version 1 monthly NPP-VIIRS data product. Monthly NPP-VIIRS data for the summer months (from May to August) at high latitudes in China were severely distorted due to stray light pollution (Zhou, Li, Zheng, et al., 2021). Therefore, appropriate integration and corrections of monthly NPP-VIIRS data are required to enhance the quality of NPP-VIIRS data.

CDEs data in this study refer to the grid data of CO_2 emissions from fossil fuel combustion, cement production, and gas flaring. As a high resolution (1000 m) CO_2 emission product, it estimated anthropic CO_2 emissions on the basis of the geographic location of global CDEs point sources and combined with multiple fuel types, such as NTL that can characterize gaseous fuels, aircraft, and fleet tracks that can characterize liquid fuels. Thus, CDEs data have been shown to be an effective representation of CO_2 emissions at different spatial scales (Oda, Maksyutov, & Andres, 2018).

Socioeconomic data were collected from China City Statistical Yearbook (2012–2018). Specific indicators include household registered population at year-end built-up area, per capita GDP, GDP of the secondary industry, secondary industry as percentage to GDP, tertiary industry as percentage to GDP, green covered area of completed area, total annual volume of passengers transported by buses and trolley buses, amount of foreign capital actually utilized, electricity consumption, local general public budget revenue, R&D personnel, and investment actually completed for real estate development.

Land cover/use data were obtained from the Chinese Academy of Sciences, Resources and Environment Science and Data Center. The data have six first-levels of land types, namely, cultivated land, forest land, grassland, water area, and unused land, and 25 secondary land types.

At last, China's administrative boundaries were obtained from the National Catalogue Service Geographic Information.

4. Methods

4.1. Quantifying UPD

The proposed UPD quantification approach mainly includes three steps (Fig. 4). The first step is to correct the NPP-VIIRS data, including annual integrations of monthly NPP-VIIRS, extractions of stable light areas, and eliminations of background noise and outliers. The second step is to extract urban areas by using the corrected NPP-VIIRS data. The third step is to calculate the SED index within urban areas for representing UPD from the corrected NPP-VIIRS data.

4.1.1. Correcting NPP-VIIRS data

Monthly data need to be integrated annually due to the lack of long time series annual NPP-VIIRS data. The raw NPP-VIIRS data did not eliminate extremely bright pixels caused by transient lights, such as firelight, gas combustion, volcano, and aurora, and background noise from low radiation detections. Thus, the specific correction steps are as follows.

- The NPP-VIIRS data for high latitudes in China from May to August were severely distorted due to stray light pollution. The data for the four months were excluded and the remaining monthly data were merged into annual data for the years 2012 to 2018 using the mean synthesis method.
- The water areas, such as lakes and reservoirs of China, were drawn on the basis of Google Earth images, and the mean light value of the water areas was taken as the minimum threshold. The areas larger than the threshold were considered to be the stable light regions. On the basis of the principle that lights in large inland waters are 0 at night, the pixel values less than the threshold were assigned 0 to eliminate unstable light sources and background noises (Tang & Cui, 2017).
- China was divided into 10 zones, and the highest light radiation value of the airport of each zone was taken as the highest threshold of that zone. The pixel larger than the threshold is regarded as the outlier pixel. An eight neighborhood algorithm was used to eliminate outliers in stable light regions. For process details, readers are advised to consult the study by Shi et al. (Shi, Yu, et al., 2014).

4.1.2. Extracting urban area

Accurate and meticulous extraction of urban areas is the basis of measuring the SED index. Currently, studies on extracting urban areas using NTL can be categorized into three main approaches, namely threshold segmentation method, edge detection method, and dynamic clustering method (Zhao, Jian, & Jwa, n.d.; Xie, Weng, & Fu, 2019; Zhao, Zhou, Li, et al., 2020; Zhou, Smith, Elvidge, et al., 2014). Among them, the threshold segmentation was regarded as a popular approach due to its simple, effective, and stable segmentation performance. Thus, combined with the corrected NPP-VIIRS data, Otsu algorithm, an optimal adaptive threshold algorithm, was used to extract urban areas in this study (Emre & Rzu, 2018; Lamphar, 2020). Otsu algorithm is an image binarization algorithm based on the principle of least squares method. This algorithm can divide the image into two types: foreground (urban area) and background (nonurban area) by calculating the threshold value of the connected areas. The specific steps are described below: first, if the value ranges of NPP-VIIRS images are [Min–Max], then we will set the threshold (T) to each value in the ranges from Min to Max. We then determined whether the pixel value is greater than T. The pixel belongs to the foreground class if the pixel value is greater than T; otherwise, it belongs to the background class and calculates the class variance (V) of the two classes. Next, the V corresponding to all T was calculated to find the largest V, where its corresponding T was the

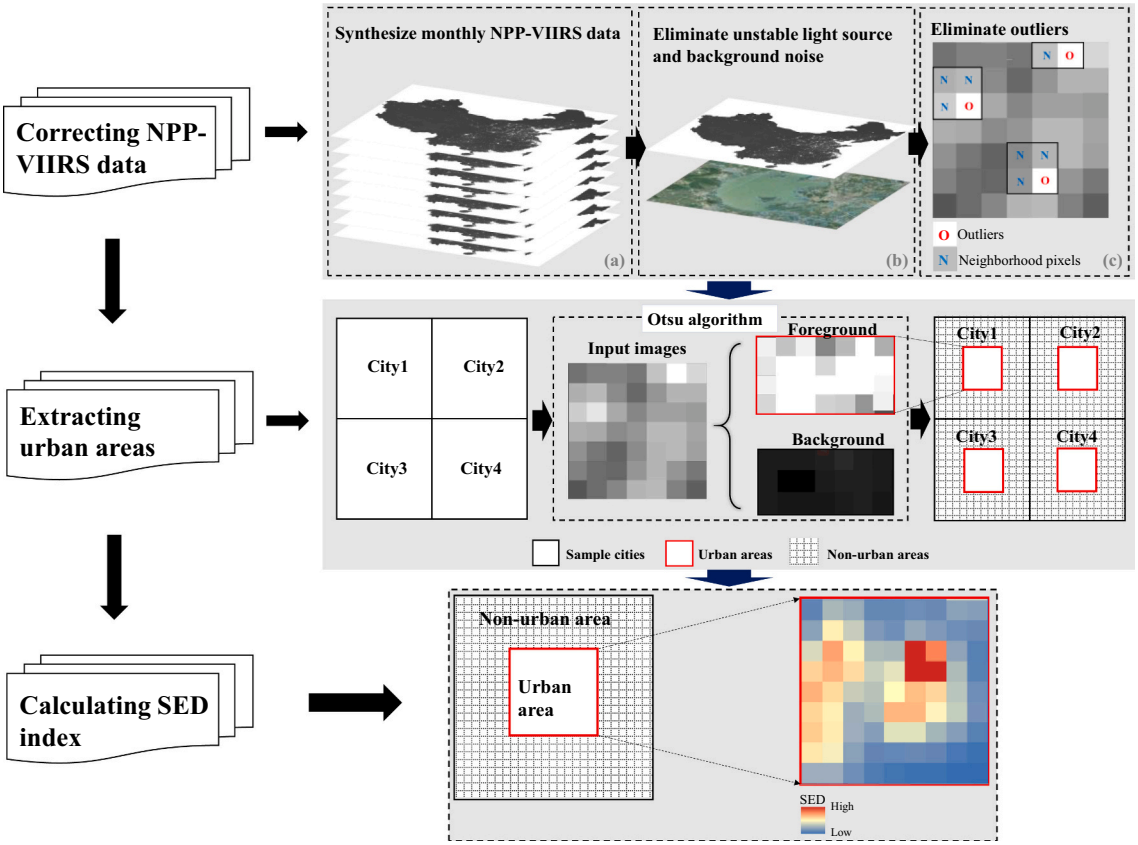

Fig. 4. Flow chart of UPD quantification.

optimal threshold. Finally, urban areas can be extracted effectively on the basis of the optimal threshold (Fig. 4).

4.1.3. Calculating SED index

Most studies at home and abroad quantify UPD on the basis of average density method (e.g., the ratio of regional population or economic output value to regional area). This method can only show the average population density or economic density at the city level but cannot identify spatial UPD differences within a city. An example is shown in Fig. 5. The average densities of City 1 and City 2 are 2, but their UPDs are different completely. Specifically, we can see that the lights of City 1 are concentrated on the right side of the city, which present a compact UPD. On the contrary, the lights of City 2 are distributed within the city evenly, which present a dispersed UPD. The average density method cannot reflect the difference in UPD. The following model was constructed to measure SED in this study (Henderson et al., 2019) and compensate for the above limitation:

$$\mathrm{SED_j} = \sum_{i}^{N_j} \mathrm{S_{ij}} \frac{\mathrm{S_{ij}}}{\mathrm{S_j}} = \mathrm{SD_j}\left[1 + \frac{\mathrm{Var(S_j)}}{\mathrm{SD_j^2}}\right] = \mathrm{SD_j}\left[1 + CV\left(S_j\right)^2\right] \quad (1)$$

where SED_j represents the SED index of city j; S_{ij} denotes the radiance of the ith grid of city j; S_j represents the sum of the radiance in the urban area of city j. SD_j is the average socioeconomic density of city j. CV is the coefficient of variation and $SD_j = \frac{\sum_i^{N_j} P_{ij}}{N_j}$. Using model (1), the SED indices of City 1 and City 2 are calculated to be 2.625 and 2, respectively. The SED distribution in City 1 is more concentrated than that in City 2, which is consonant with the expected results in Fig. 5.

4.2. Developing benchmark regression model

The following benchmark regression model was developed to identify EUC accurately.

$$lnCDE_{it} = \alpha + \beta\, lnSED_{it} + \theta\,(lnSED_{it})^2 + \gamma\, lnX_{it} + \eta_{it} \quad (2)$$

where i is the city; t is the year; CDE is measured by the total annual CDEs within urban area. SED is the core explanatory variable. $(SED)^2$ reflects the nonlinear relationship of EUC as truly as possible. X represents the control variables, including population density (PD, *ratio of total population to area of municipal districts*) (Liu et al., 2021), population size (POP, *household registered population at year-end of municipal districts*) (Shi et al., 2021), GDP per capita (PGDP, per capita *GDP of municipal districts*) (Liang et al., 2021), GDP of secondary industry (GDP2, *GDP of the secondary industry of municipal districts*) (Liu et al., 2021), proportion of secondary and tertiary sectors in GDP (SEC, *the sum of secondary industry as percentage to GDP and tertiary industry as percentage to GDP of municipal districts*) (Zhao et al., 2021), and greening degree (UG, *green covered area of completed area of municipal districts*) (Yao, Kou, Shao, et al., 2018) (Table S2). η is the random perturbation term. All indices are transformed logarithmically to minimize the effect of unit dimensions and heteroscedasticity.

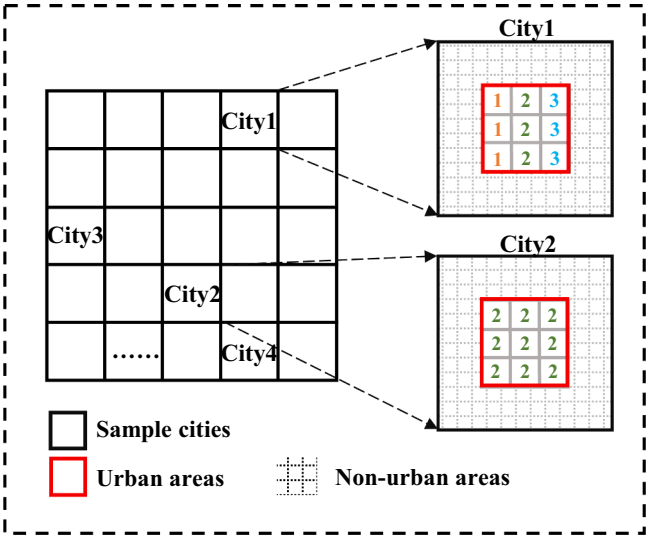

Fig. 5. Spatial distributions of NTL within urban areas. Note: the values in the red boxes can intuitively identify compact or dispersed UPDs. (For interpretation of the references to colour in this figure legend, the reader is referred to the web version of this article.)

The explained variables that lag one stage was added into the model to eliminate the effect of endogenous variables in the static panel data model as much as possible. Thus, the regression model (2) can be redeveloped as the following dynamic panel data, and the *system generalized method of moment* (GMM) was used for estimations.

$$lnCDE_{it} = \alpha + \lambda\, lnCDE_{i,t-1} + \beta\, lnSED_{it} + \theta\,(lnSED_{it})^2 + \gamma\, lnX_{it} + \mu_{it} + \eta_{it} \quad (3)$$

where $CDE_{i,t-1}$ is the lagging one-stage CDE.

5. Results

5.1. NPP-VIIRS data correction evaluation

As described above, the radiance values of the raw monthly NPP-VIIRS data are unstable and scattered, resulting in data incompatibility. Specifically, the radiation values present a strong fluctuation within different monthly NPP-VIIRS data in 2012 and 2018. After annual correction, the data have a good continuity, which is suitable for long-term time series analysis (Fig. 6). The evaluation revealed that the correction completely eliminates the outliers and background noise (Fig. 7), which can ensure the reliability of UPD quantification results. For example, the light radiation values of Aksu in Xinjiang Province and Fu in Shaanxi Province changed from 1013.07 and 1100.04 $nWcm^{-2}sc^{-1}$ before correction to 136.61 and 156.33 $nWcm^{-2}sc^{-1}$, respectively (Fig. 7). The corrected NPP-VIIRS data can provide a long time series (2012–2018) and large-scale data sources for the exploration of EUC in China. The data have rich socioeconomic spatial information and compensate the deficiencies of no spatial details and the one-dimensionality for traditional statistic data and optical remotely sensed data.

5.2. Urban area extraction evaluation

Verifications of visual comparison and confusion matrix were used to test urban area extraction accuracy in this study. Some typical cities (Beijing, Shanghai, Guangzhou, and Shenzhen) were selected to visually compare the spatial similarities and differences between the urban areas extracted on the basis of the Otsu algorithm and Google Earth images. Taking Beijing as an example, the Otsu algorithm can effectively identify the six urban districts and most of the new areas of urban development. The urban and marginal areas were effectively identified in Shanghai, Guangzhou, and Shenzhen (Fig. 8). Taking land use/cover data in 2010, 2015, and 2018 as the verification data, different sizes of cities were selected randomly to verify the accuracy of extraction results in urban areas on the basis of the confusion matrix approach. The accuracy verification results proved that urban areas can be extracted efficiently and accurately on the basis of the Otsu algorithm by using the NTL (Tables S3–S4).

5.3. China's UPD evaluation

The spatiotemporal characteristics of SED in China are shown in

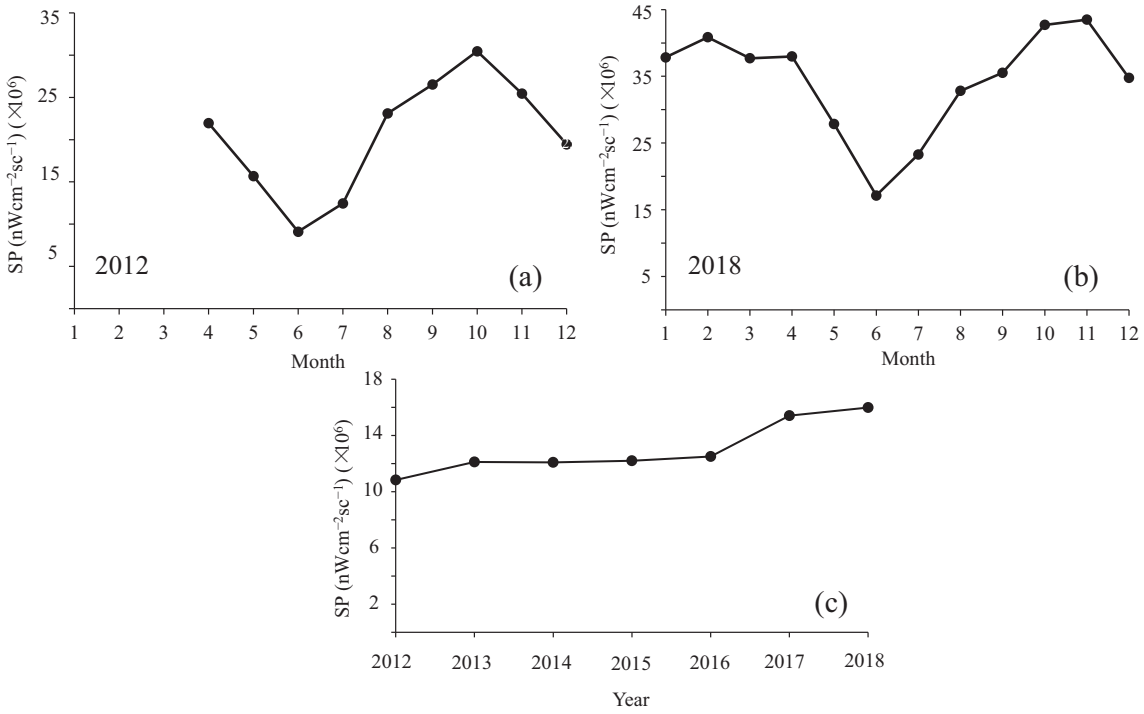

Fig. 6. Comparisons of radiance values between raw monthly data and corrected annual data. Note: SP is the total of pixel radiances. (a) and (b) are the total of monthly pixel radiances before correction of NPP-VIIRS data in 2012 and 2018, respectively; (c) is the total of annual pixel radiances after correction in 2012–2018. The monthly data were combined as annual data using the mean synthesis method.

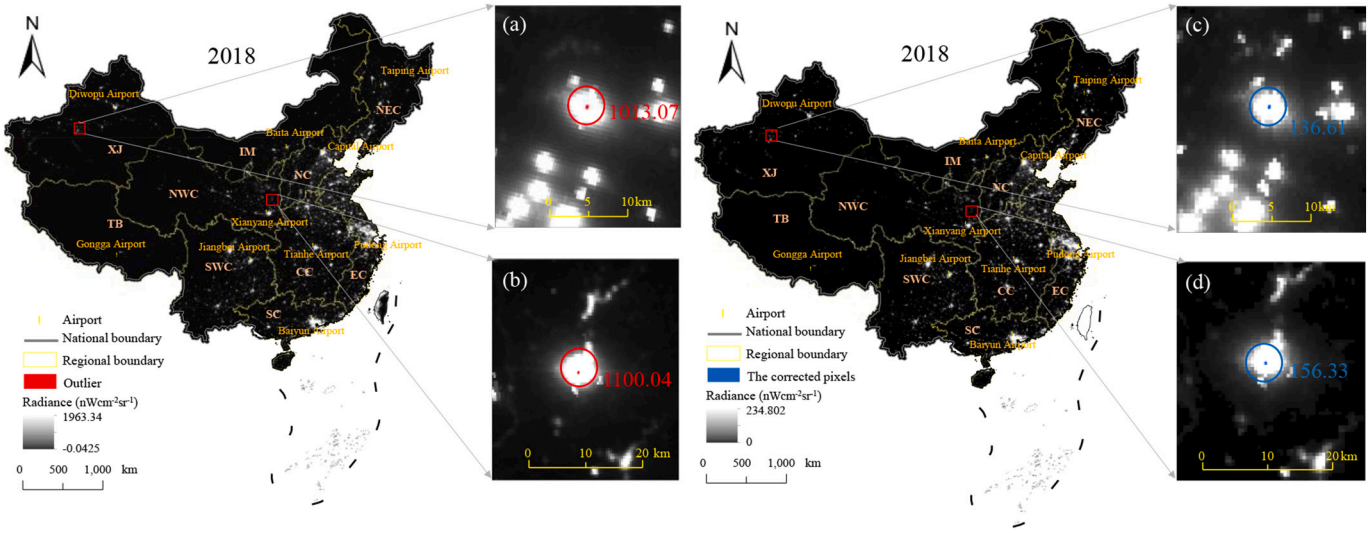

Fig. 7. Comparisons of the raw and corrected NPP-VIIRS data for China in 2018. Note: (a)–(b) raw NPP-VIIRS data; (c)–(d) corrected NPP-VIIRS data.

Fig. 9. The definition spacing method was adopted to classify the SED into four levels: high SED (>40), medium-high SED (30–40), medium SED (20−30), and low SED (0−20). This process was performed to distinguish spatial differences. From 2012 to 2018, the SED presents a stable spatial pattern. Urban areas with SED > 30 are mainly located in the northeast region and eastern coastal region. This condition may be attributed to the high level of urbanization, the developed transport links, the excellent infrastructure, the high population density and the high intensity of socioeconomic activities in the eastern coastal areas. Northeast region has perfect technology and infrastructure, rich resources and energy, and high urbanization level, resulting in more concentrated socioeconomic development (Hu, Li, & Dong, 2021). Most of the SED in the cities of central region are at a medium level. Although the development of urbanization can promote the resource agglomeration in central region. Although the level of socio-economic development in the central region has been rising continuously in recent years, the excessive rate of urban sprawl has pulled down the overall SED. The low SED is concentrated south of the central region. For example, Yongzhou, Shaoguan, and Wuzhou, which have small urban areas and low levels of socioeconomic development, hence low overall SED. Different SED levels are observed in the southwest region. This condition is because highly developed cities and poor and backward areas are found in the southwest region.

The SEDs in large cities, medium-sized cities, and small cities present “wave-like” weak growths from 2012 to 2018 (Fig. 10), which are attributed to the “polarization-diffusion effect”. Specifically, cities with

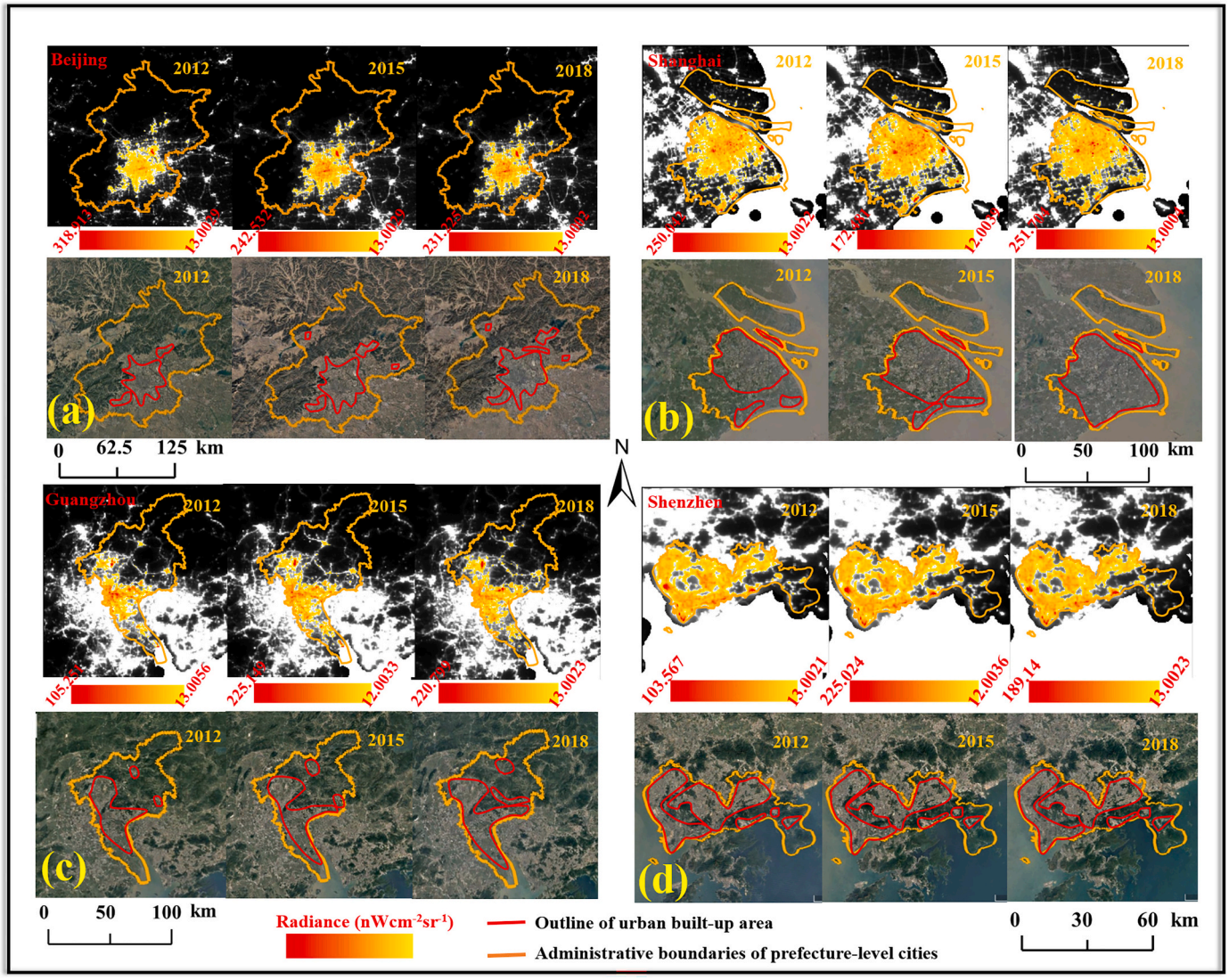

Fig. 8. Visual comparisons between urban areas extracted by the Otsu algorithm and Google Earth images.

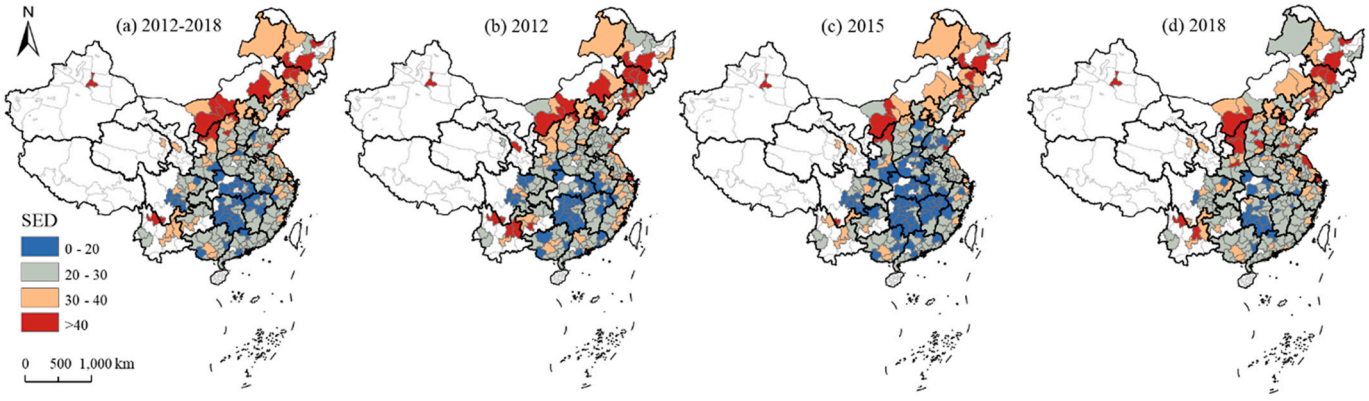

Fig. 9. Spatiotemporal trends of SEDs in China from 2012 to 2018.

better development conditions take the lead in driving local socioeconomic development and form a clustering trend within the region in pursuit of scale and agglomeration benefits. The agglomeration will attract more production factors to gather, which is called the "polarization effect" (Ye, Zhu, Li, et al., 2018). When the degree of agglomeration reaches the maximum tolerance of economic capacity and environmental capacity, it will lead to a series of urban problems like transport congestion, ecological contamination, large demand for public facilities, energy shortage, public security disorder, and unbalanced development between regions. The government will take a series

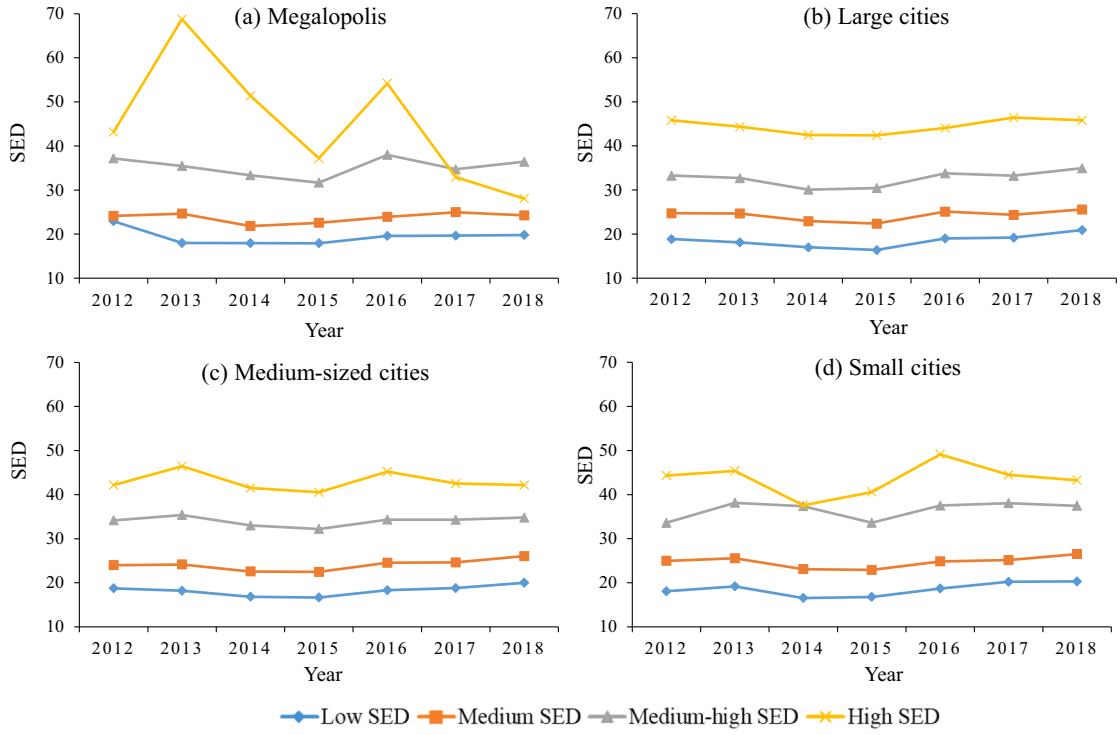

Fig. 10. Spatiotemporal trends of SEDs in cities within different sizes.

of interventions, such as environmental regulation and industrial regulation, to avoid these problems, and the population and industries will start to move to the suburbs, resulting in economic diffusion and weakening of SEDs (Liu, Pan, Hou, et al., 2020). However, in megalopolis cities, the SED at a high level presents a fluctuating decrease (Fig. 10 (a)). The socioeconomic factors, such as labors and industries, tend to shift to the suburbs with lower cost because the environment, traffic pressure, and the cost of living in megalopolis are relatively high. The more developed rail transit system in megalopolis cities makes it more convenient and cheaper for people to travel, leading to a relative

Table 1
Effects of SED on CDEs: benchmark regression results.

Variable	(1)	(2)	(3)	(4)	(5)	(6)
	OLS	OLS	FE	FE	GMM	GMM
L.ln*CDE*					0.994***	1.070***
					(451.60)	(154.58)
ln*SED*	8.801***	4.556***	9.201***	5.315***	0.129***	0.464***
	(6.00)	(4.21)	(6.22)	(5.00)	(2.71)	(8.42)
(ln*SED*)2	−1.240***	−0.654***	−1.296***	−0.768***	−0.016**	−0.061***
	(−5.61)	(−4.00)	(−5.82)	(−4.79)	(−2.14)	(−7.35)
ln*PD*		−0.090***		−0.095***		−0.738***
		(−3.74)		(−4.08)		(−10.57)
ln*POP*		0.584***		0.577***		−0.010**
		(21.28)		(21.56)		(−2.20)
ln*PGDP*		0.348***		0.419***		0.010**
		(9.44)		(11.41)		(2.41)
ln*GDP2*		4.011***		3.794***		0.088**
		(12.32)		(11.92)		(2.51)
ln*SEC*		8.359***		8.347***		0.118*
		(13.69)		(14.03)		(1.77)
ln*UG*		−0.246***		−0.210**		0.024***
		(−2.72)		(−2.38)		(5.34)
Constant	−0.090	−21.370***	−0.808	−22.415***	−0.159*	1.546***
	(−0.04)	(−8.66)	(−0.33)	(−9.27)	(−1.81)	(5.05)
Time effect	No	No	Yes	Yes		
Observations	1799	1773	1799	1773	1542	1516
Sample city	257	257	257	257	257	257
F value	45.91	226.6	12.11	143.3		
F test	0	0	0	0		
Sargan test					0.120	0.179
R^2	0.049	0.507	0.051	0.533		

Note: L.ln*CDE* is the log-lagged one period CDE; ***, **, and * represent 1%, 5%, and 10% significance levels respectively; *T* statistic values are in parentheses; F test and Sargan test are the *p* values.

decrease in the SED in megacities.

5.4. Benchmark regression result analysis

Benchmark regression results are listed in Table 1. All *p*-values for the Sargan test are >0.1, indicating that the GMM model is accurate and reasonable (Liu et al., 2021). Table 1 also lists the *ordinary least squares* (OLS) results and the *fixed effects model* (FE) results as references, but the GMM results are used as the final basis. The GMM results in column (5) indicate SED's estimator is 0.129, which is significance positive at the 1% level, meaning an increment in the compactness of UPD will aggravate CDEs. The estimator of $(SED)^2$ is −1.240, which is of negative significance at the 1% level, indicating that the relationship of UPD and CDEs presents an inverse U-shaped curve, and the inflection point of the curve is 4.031. In other words, when the logarithm of SED is <4.031, the increase in UPD can increase CDEs. When the logarithm of SED exceeds 4.031, the increase in UPD will reduce CDEs. The control variable was added in column (6) to reduce the interference of other factors as much as possible. The SED's estimator is 0.464, significance at the 1% level, implying the increase in UPD still aggravates CDEs. The estimator of $(SED)^2$ is −0.061, which is significance at the 1% level, indicating that the UPD still presents an inverse U-shaped curve relationship with CDEs, and the inflection point of the curve is 3.803. The increase in SED increases CDEs. This condition is because at the beginning of the agglomeration, public service, infrastructure, science and technology input, and environmental governance fail to keep pace with the concentration rate of population scale and expansion rate of production scale, which bring some problems with urban transport congestion and ecological contamination (Cheng, 2016). At this time, the concentration of negative externalities plays a leading role. However, SED's continuous increase leads to the scale effect and spillover effect of agglomeration. When SED reaches the inflection point value of the inverse U-shaped curve, the positive externality of agglomeration plays a leading role and CDEs decrease (Wang & Wang, 2019). Columns (1)–(4) show the estimates of OLS and FE to verify the credibility of the results. The estimation results of OLS and FE show a significant inverse U-shaped curve relationship between UPD and CDEs, which is consonant with the GMM results. On the whole, EUC shows an inverse U-shaped curve. CDEs increase with the increase in compactness of UPD. When the compactness reaches a certain degree, that is, exceeds a certain inflection point value, CDEs gradually reduce.

The analysis of the effect of control variables on CDEs is conducive to propose more targeted suggestions because control variables affect CDEs. For the control variables in column (6), the estimator of lnPD and lnPOP are −0.738 and − 0.010 respectively, significance at the 1% level, indicating that CDE decreases as increasing population density and population size. The scale effect and agglomeration effect generated by high population density inside cities are conducive to sharing urban public infrastructure and services, promoting the formation of agglomeration economy, improving urban production efficiency, and reducing CDEs (Wang & Huang, 2019). The estimator of lnPGDP is 0.010, significance at the 1% level, indicating economic development can increase CDEs. At present, China's economic development is fast, and energy-intensive products have a large demand, leading to the increase in CDEs by stimulating energy consumption (Wang & Huang, 2019). The estimator of lnGDP2 is 0.088, which is significant at the 1% level, indicating that industrial polluting gases are one of the reasons for CDE's aggravation. The estimator of lnSEC is 0.118, which is significant at the 1% level, indicating that the increase in the GDP of secondary and tertiary industries aggravates CDEs. The estimator of lnUG is 0.024, which is significant at the 1% level, indicating that the increase in green coverage rate can aggravate the cause of CDEs. Although the improvement of greening degree is conducive to decrease CDEs, the results are contrary in this study. On the one hand, it may be because the time lag effect of greening degree on CDEs is not fully considered when selecting the control variable. Greening degree in the current period is likely to inhibit CDEs in the next period. On the other hand, urban greening is possibly reflected in urban areas and often goes hand in hand with CDEs, thereby creating the illusion that greening degree is correlated with CDEs positively, which is consonant with the study conclusions of Shi et al. (Shi, Wang, et al., 2019).

5.5. Robustness test analysis

The control variable substitution method and the typical city elimination method were adopted to conduct the robustness test for testing the credibility of the benchmark regression results (Table 2). First, lnGDP2 was replaced by GDP of tertiary industry (lnGDP3) for the robustness test. Columns (1)–(3) show that the positive and negative signs and significance of the SED's estimator are consonant with benchmark regression results, meaning EUC still presents an inverse U-shaped curve. Similarly, the inflection point value of the curve is 3.820 in the GMM regression results in column (3), which is consonant with benchmark regression results. Second, in view of its high autonomy in administrative power and high degree of economic development, the municipality has a more prominent status and role than other cities in China. Thus, (4)–(6) are listed as the robustness test excluding the four municipalities. The results show that the positive and negative signs and significance of SED's estimator are still consonant with benchmark regression results. The inflection point value of the curve is 3.814 in the (6) GMM regression results, which is consonant with the benchmark regression results. An inverse U-shaped curve is found on EUC through the above robustness test.

6. Discussion

6.1. SED index evaluation

The SED index constructed for quantifying UPD was in similarity to available studies. From a land use/cover perspective, Wang et al. (Wang et al., 2019a) and Shi et al. (Shi, Li, Chen, et al., 2019) identified compact urban structures within some developed cities in China. Similarly, many megalopolises show high SED in our study (Fig. 9). Gao et al. (Gao, Huang, He, et al., 2016) identified a large number of low-density cities in backward regions by calculating the 2000 and 2010 population indices, which are extremely close to our study. We found that the U-shaped curve of EUC is similar to that of Chen et al. (Chen et al., 2020) by testing the effect of UPD. They concluded that agglomerations have a significance inverse U-shaped curve in relation to wastewater emissions, sulfur dioxide emissions, and soot emissions.

Compared with previous indicators accompanied by 1D and nonspatial characteristics, the SED index derived from NTL can accurately represent the spatial distribution differences in socioeconomic activities from multidimensions. The SED index can effectively identify the vertical development model, compensating for the shortcomings of the average density method (Fig. 5). Taking Beijing as an example, a sample line from west to east was established to clearly show the gradient change in UPD (Fig. 11). A comparison between the profile and Google Earth image shows that SED is highest in the urban center, decreasing from the urban center to the periphery. Thus, the use of NPP-VIIRS data to develop SED index can update the dynamic development of UPD in real time and improve the accuracy of UPD quantification results with finer spatial resolution.

6.2. Heterogeneity analysis

As listed in Table 1, EUC presents an inverse U-shaped curve in accordance with the results of benchmark regression results. Considering the differences of city sizes, heterogeneity analysis was conducted to identify nonlinear relationships (Table S5). Furthermore, an additional complementary experiment was conducted to analyze the effect of population density on CDEs (Liang et al., 2021) based on the whole

Table 2
Robustness tests of the effects of SED on CDEs.

Variable	(1)	(2)	(3)	(4)	(5)	(6)
	OLS	FE	GMM	OLS	FE	GMM
L.ln*CDE*			1.067***			1.069***
			(154.10)			(143.52)
ln*SED*	3.799***	4.657***	0.466***	4.726***	5.469***	0.450***
	(3.48)	(4.38)	(8.46)	(4.32)	(5.09)	(8.15)
(ln*SED*)2	−0.542***	−0.672***	−0.061***	−0.683***	−0.793***	−0.059***
	(−3.28)	(−4.19)	(−7.36)	(−4.14)	(−4.89)	(−7.07)
ln*PD*	−0.065***	−0.079***	−0.689***	−0.099***	−0.104***	−0.660***
	(−2.73)	(−3.42)	(−9.86)	(−4.00)	(−4.31)	(−9.55)
ln*POP*	0.543***	0.541***	−0.014***	0.577***	0.576***	−0.010**
	(19.91)	(20.49)	(−3.43)	(19.42)	(19.87)	(−2.29)
ln*PGDP*	0.457***	0.521***	0.014***	0.341***	0.412***	0.005
	(13.29)	(15.42)	(3.55)	(9.14)	(11.06)	(1.26)
ln*GDP3*/ln*GDP2*	2.179***	2.292***	−0.043**	4.057***	3.829***	0.085**
	(10.60)	(11.51)	(−2.50)	(12.33)	(11.88)	(2.43)
ln*SEC*	−2.958***	−2.724***	0.033	8.391***	8.380***	0.107
	(−7.46)	(−7.09)	(0.98)	(13.64)	(13.96)	(1.61)
ln*UG*	−0.182**	−0.153*	0.024***	−0.242***	−0.198**	0.025***
	(−2.00)	(−1.74)	(5.47)	(−2.65)	(−2.21)	(5.53)
Constant	−3.039*	−5.573***	1.872***	−21.689***	−22.735***	1.209***
	(−1.67)	(−3.13)	(6.99)	(−8.69)	(−9.30)	(4.07)
Time effect	No	Yes		No	Yes	
Observations	1773	1773	1516	1745	1745	1492
Sample city		257	257			253
F value	217.4	141.9		187.3	119.0	
F test	0	0		0	0	
Sargan test			0.143			0.325
R^2	0.496	0.531		0.463	0.491	

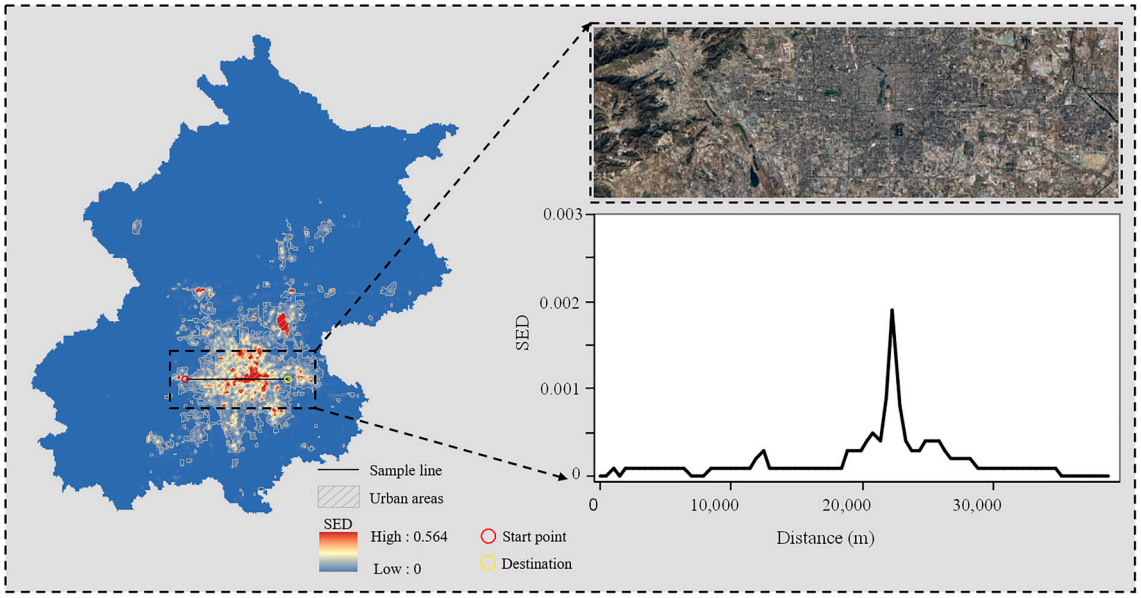

Fig. 11. SED profile in Beijing.

country and different city sizes since SED is not the only indicator affecting CDEs, replacing the core explanatory variables and keeping the model and control variables unchanged, and the results are presented in the supplementary information (Table S6).

For medium-sized and small cities, the estimator of SED at the 1% level is significantly positive, while the estimator of $(SED)^2$ at the 1% level is significantly negative (Table S5). The results show that the EUC of medium-sized and small cities presents an inverse U-shaped curve, which is consonant with benchmark regression results. For megalopolis, the estimator of SED and the estimator of $(SED)^2$ are −0.299 and 0.038, respectively, significance at the 10% level. The results show that the EUC of megalopolis is U-shaped curve, which is contrary to the benchmark regression results. For large cities, the results are insignificant. Medium-sized and small cities have relatively few polluting enterprises, less demand for public infrastructure, and shorter transportation distances. The socioeconomic size of medium-sized and small cities is small. As the compactness of the UPD increases, the agglomeration effect gradually changes from negative externalities to positive externalities, playing an important role in improving urban environmental quality and reducing CDEs (Huang, Hong, & Ma, 2020). Megalopolis, such as Beijing, Wuhan, and Shanghai, are highly attractive to migrants. Benefiting from the scale effect and agglomeration effect of high economic agglomeration brought by high population density, promoting the sharing of urban public infrastructure and

services, knowledge spillover, and labor pool effect can improve urban production efficiency and reduce CDEs. However, high urban population density leads to overcrowding, increased costs of various types of competition, traffic congestion, and excessive demand for infrastructure and operation and maintenance, thereby increasing CDEs (Wang & Huang, 2019). Large cities' SED is at a low level, and the overall CDEs are large. Thus, fully reflecting the positive externality effect of agglomeration economy is difficult.

As can be seen from Table S6, overall (column (1)), the coefficient on LSD is significantly positive and the coefficient on $(LSD)^2$ is significantly negative, indicating that there is also an inverted U-shaped relationship between LSD and CDEs. Based on the results of the baseline regressions for cities of different sizes (columns (2)–(5)), it can be seen that the LSDs of medium cities also show a significant inverted U-curve relationship with CDEs, and conversely, the LSDs of megacities show a significant U-curve relationship with CDEs. The regression results for large and small cities were not significant. From the above analysis, we know that LSD is also another important factor affecting CDEs. An in-depth investigation into the reasons why LSD affects CDEs will be the focus of our future research.

6.3. EUC transmission factor assessment

Several studies have attempted to explore EUC. However, most of them have not systematically analyzed the transmission factors. Correspondingly, we attempted to assess EUC transmission factor from the following aspects (Fig. 12). First, bus passenger volume may be one of the transmission factors of EUC. People's commuting distance and time are shortened by the compact economic activities within the urban area, making people inclined to use more low-carbon and environmentally friendly public transportation (Liang et al., 2021). However, compact economic activities can stimulate travel demand by increasing the density of regional roads, thereby increasing CDE (Wang & Huang, 2019). Compact economic activity can also aggravate traffic congestion without contributing to energy saving and emission control (Wang & Huang, 2019). Second, energy consumption may be another transmission factor of EUC. Compact economic activities are conducive to centralized energy supply and use, which can reduce CDEs (Wilson, 2013). However, excessive compact economic activity will inhibit the improvement of energy efficiency, aggravate energy consumption, and increase CDEs (Li & Ma, 2021). Third, foreign direct investment was considered an EUC's transmission factor. The scale effect and spillover effect of socioeconomic agglomeration increase with the increase in foreign investment level, which can reduce CDEs (Zhao et al., 2021).

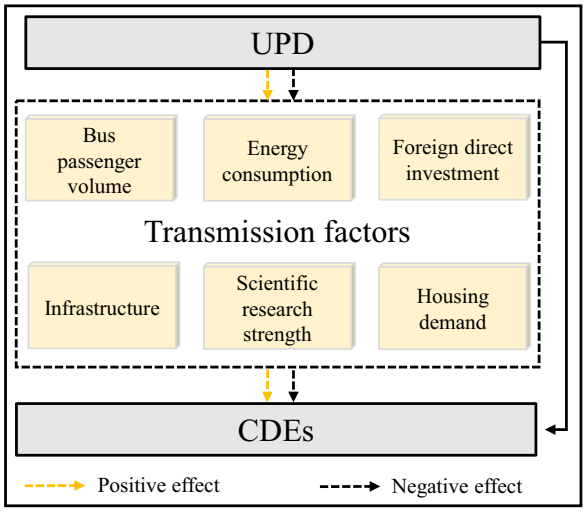

Fig. 12. Transmission factors of EUC.

However, the entry of foreign investors will lead to the 'pollution haven' and aggravate CDEs due to the low intensity of environmental regulations in developing countries (Zhao, Cao, & Ma, 2020). Fourth, infrastructure may be crucial in the transmission process of EUC. Compact economic activity is conducive to saving space and realizing the sharing of infrastructure within the region, so as to save energy consumption (Sperling & Ramaswami, 2013). However, the compact UPD leads to excessive demand for infrastructure, which brings high operation and maintenance costs, and is unconducive to energy saving and emission control (Wang & Huang, 2019). Fifth, scientific research strength was inferred to be another transmission factor. High SED can share factors, learning, and other channels within the region to improve the efficiency of human capital and then achieve energy saving and emission reduction by improving scientific research strength (Wang & Huang, 2019). However, CDEs will increase if scientific research strength is developed in the direction of improving production efficiency and expanding production scale (Wang & Huang, 2019). Sixth, UPD may affect housing demand, thereby affecting CDEs. Agglomeration can stimulate the local housing demand. Real estate developers meet more people' housing demand by reducing single-family buildings and increasing high density residential area with multiple units. The demand for lighting, heating, and cooling of air conditioning will be reduced because of the reduction in per capita housing area; thus, CDEs will be reduced correspondingly (Qin & Wu, 2015). However, a large amount of building materials and electricity energy will be consumed in the process of real estate development, which can aggravate CDEs (Wang & Huang, 2019).

Overall, the final transmission effects of these factors depend on the trade-off between their positive and negative effects. Whether EUC can be interpreted by bus passenger volume, energy consumption, foreign direct investment, infrastructure, scientific research strength, and housing demand needs further quantitative investigation. Six factors, namely, bus passenger volume (measured by total annual volume of passengers transported by buses and trolley buses) (Liang et al., 2021), energy consumption (measured by annual electricity consumption) (Yao et al., 2018), foreign direct investment (measured by foreign capital actually utilized) (Liang et al., 2021), infrastructure (measured by local general public budget revenue) (Sperling & Ramaswami, 2013), scientific research strength (measured by R&D personnel) (Yao et al., 2018), and housing demand (measured by investment actually completed for real estate development) (Liu et al., 2021), were selected in this section to examine the transmission mechanism (Fig. 12). The mediation model was used to test the transmission mechanism of EUC in this section. Details of the intermediate effects model and model testing steps are given in Yao et al. (Yao et al., 2018)

As shown in Table S7, the estimator of SED and the estimator of $(SED)^2$ are significant in column (1). In column (2), SED's estimator is significantly positive, and the estimator of $(SED)^2$ is significantly negative, indicating that the relationship between UPD and BPV presents an inverse U-shaped curve. In column (3), a significant positive correlation is found between bus passenger volume and CDE, and CDE increases by approximately 0.022 units when bus passenger volume increases by one unit. Thus, the mediating effect holds. In column (3), SED's estimator is significantly positive, and the estimator of $(SED)^2$ is significantly negative, indicating that a partial intermediary effect is found, that is, UPD can reduce CDEs by influencing bus passenger volume. The higher the degree of urban agglomeration, the more concentrated the transportation network and services, and the more centralized the residents' travel, which is conducive to increasing the scale effect and reducing CDEs (Liang et al., 2021). In column (4), the estimator of SED is significantly positive, whereas the estimator of $(SED)^2$ is significantly negative, indicating that the relationship between UPD and energy consumption presents an inverse U-shaped curve. In column (5), the relationship between energy consumption and CDEs is positive at the significance level of 1%. For every increase in energy consumption by 1 unit, CDE increases by approximately 0.026 units, indicating that the mediation effect is established. The estimator of SED in column (5) is

significantly positive, and the estimator of $(SED)^2$ is significantly negative, indicating the existence of a partial mediation effect. The per capita housing area decreases with the increase in the compactness of the city. Thus, the demand for lighting and air conditioning will be smaller, the heat dissipation of the house will be reduced, and the energy consumption will be relatively reduced (Holden & Norland, 2005). The effect of foreign direct investment on CDEs is insignificant. Thus, the transmission path that UPD can affect CDEs through foreign direct investment may not be established.

As shown in Table S8, partial mediating effects are found in infrastructure and housing demand. EUC is still an inverse U-shaped curve through the transmission of mediators of infrastructure and housing demand. A more compact UPD is conducive to realizing intraregional infrastructure sharing, reducing regional energy costs, and reducing CDEs (Wang & Huang, 2019). housing demand increases when the population becomes denser, and real estate developers try to meet the demand of more people by reducing the number of single-family buildings and increasing the number of high-rise apartments with multiple units. With the decrease in per capita housing, the demand for lighting, heating, and cooling of air conditioning decreases, thereby reducing CDEs (Qin & Wu, 2015). The effect of scientific research strength on CDEs is insignificant. Thus, the transmission path that UPD can affect CDEs by influencing scientific research strength may be invalid.

7. Conclusions

257 prefecture-level cities in China were taken as study samples to analyze EUC from the perspective of SED approach in this study. First, the SED index was constructed to measure UPD on the basis of the corrected NPP-VIIRS data. Then, EUC was analyzed by establishing a benchmark regression model. The results show that the SED index can effectively measure UPD with rich spatial information from multiple dimensions in China. EUC presents an obvious inverse U-shaped curve in China. When SED is lower than the inflection point value, SED's negative externality is significant, but the positive externality is insufficient, and the increase in compactness of UPD aggravates CDEs. With the passage of time, the agglomeration's positive externalities start to appear. When SED exceeds the inflection point value, the agglomeration's positive externalities are greater than its negative externalities, thereby reducing CDEs. The robustness test shows that the compactness of UPD still presents a significance inverse U-shaped curve relationship with CDEs. Significant heterogeneity is found in EUC. There is an inverse U-shaped curve in small and medium-sized cities while a U-shaped curve is presented in megalopolis. Bus passenger volume, energy consumption, infrastructure, and housing demand are proven as the transmission factors of EUC.

A few limitations were identified in our study that will have to be resolved in future studies. Some natural factors affecting CDE dispersion, such as wind direction, wind speed, precipitation, and temperature, were ignored in this study. In future studies, the spatial proximity effect of economic activities and natural factors will be fully considered on the basis of finer resolution and longer timing. We did not identify the diversity of UPD, such as single-centered, multi-centered UPD, and concentric UPD. More effective approaches will be developed to quantify multiple types of UPD and their effects.

Furthermore, as cities are complex systems, traditional linear science has limitations for a better knowledge and understanding of cities (Gong, Xu, Jiao, et al., 2021). The urban scalar law provides a simple method for studying complex urban systems (Lei, Jiao, Xu, et al., 2021a; Lei, Jiao, Xu, et al., 2021b). Many urban socioeconomic indicators, such as GDP, crime, household electricity consumption, road length, etc., are often included in the urban indicator system to examine whether they follow the urban scalar law (Ramaswami, Jiang, Tong, et al., 2018). However, urban environmental indicators, such as CDEs, haze pollution, etc., are rarely used. In the future, we may combine nighttime lighting data, CDEs grid data and other high resolution spatiotemporal data to investigate whether CDEs follow urban scalar rates at different levels (e.g. city-level as well as intra-city cell level).

CRediT authorship contribution statement

Shirao Liu: Writing – original draft, Methodology, Validation. **Jingwei Shen:** Methodology, Validation. **Guifen Liu:** Editing, Validation. **Yizhen Wu:** Conceptualization, Validation, Editing. **Kaifang Shi:** Conceptualization, Methodology, Supervision, Editing.

Acknowledgements

This work was supported by the National Natural Science Foundation of China (42101345) and the Chongqing Social Science Planning Project (2021NDQN39).

Appendix A. Supplementary data

Supplementary data to this article can be found online at https://doi.org/10.1016/j.compenvurbsys.2022.101847.

References

Chen, C., Sun, Y., Lan, Q., et al. (2020). Impacts of industrial agglomeration on pollution and ecological efficiency-A spatial econometric analysis based on a big panel dataset of China's 259 cities[J]. *Journal of Cleaner Production, 258*, Article 120721.
Cheng, Z. (2016). The spatial correlation and interaction between manufacturing agglomeration and environmental pollution[J]. *Ecological Indicators, 61*, 1024–1032.
Chien, S. S. (2010). *Prefectures and prefecture-level cities: the political economy of administrative restructuring[M]*.
Ciccone, A., & R. H.. (1996). Productivity and the density of economic activity[J]. *American Economic Review, 86*(1), 54–70.
Dong, F., Wang, Y., Zheng, L., et al. (2019). Can industrial agglomeration promote pollution agglomeration? Evidence from China[J]. *Journal of Cleaner Production, 246*, Article 118960.
Emre, Y., & Rzu, E. A. (2018). Examining urbanization dynamics in Turkey using DMSP–OLS and socio-economic data[J]. *Journal of the Indian Society of Remote Sensing, 46*.
Gao, B., Huang, Q., He, C., et al. (2016). How does sprawl differ across cities in China? A multi-scale investigation using nighttime light and census data[J]. *Landscape and Urban Planning, 148*(41), 89–98.
Gong, J., Xu, G., Jiao, L., et al. (2021). Urban scaling law and its application[J]. *Acta Geographica Sinica, 76*(02), 251–260 (in Chinese).
Guo, Y., Tong, L., & Mei, L. (2020). The effect of industrial agglomeration on green development efficiency in Northeast China since the revitalization[J]. *Journal of Cleaner Production, 258*, Article 120584.
Hankey, S., & Marshall, J. (2010). Impacts of urban form on future US passenger-vehicle greenhouse gas emissions[J]. *Energy Policy, 38*(9), 4880–4887.
Henderson, J. V., Nigmatulina, D., & S. K.. (2019). Measuring urban economic density [J]. *Journal of Urban Economics, 125*, Article 103188.
Holden, E., & Norland, I. T. (2005). Three challenges for the compact city as a sustainable urban form: Household consumption of energy and transport in eight residential areas in the Greater Oslo Region[J]. *Urban Studies, 42*(12), 2145–2166.
Hu, X., Li, L., & Dong, K. (2021). What matters for regional economic resilience amid COVID-19? Evidence from cities in Northeast China[J]. *Cities, 103440*.
Huang, Y., Hong, T., & Ma, T. (2020). Urban network externalities, agglomeration economies and urban economic growth[J]. *Cities, 107*, Article 102882.
Kahn, M. E. (2009). Urban growth and climate change[J]. *Annual Review of Resource Economics, 1*(1), 333–350.
Lamphar, H. (2020). Spatio-temporal association of light pollution and urban sprawl using remote sensing imagery and GIS: A simple method based in Otsu's algorithm [J]. *Journal of Quantitative Spectroscopy and Radiative Transfer, 253*, Article 107068.
Lei, W., Jiao, L., Xu, G., et al. (2021b). Urban scaling in rapidly urbanising China[J]. *Urban Studies, 00420980211017817*.
Lei, W., Jiao, L., Xu, Z., et al. (2021a). Scaling of urban economic outputs: insights both from urban population size and population mobility[J]. *Computers, Environment and Urban Systems, 88*, Article 101657.
Li, X., & Ma, D. (2021). Financial agglomeration, technological innovation, and green total factor energy efficiency[J]. *Alexandria Engineering Journal, 60*(4), 4085–4095.
Liang, C., Liu, X., & Li, S. (2021). Urban spatial development mode and smog pollution - Based on the perspective of population density distribution [J]. *Economic Perspectives, 2*, 80–94.
Liu, S., Shi, K., Wu, Y., et al. (2021). Remotely sensed nighttime lights reveal China's urbanization process restricted by haze pollution[J]. *Building and Environment, 206*, Article 108350.
Liu, T., Pan, S., Hou, H., et al. (2020). Analyzing the environmental and economic impact of industrial transfer based on an improved CGE model: Taking the

Beijing–Tianjin–Hebei region as an example[J]. *Environmental Impact Assessment Review, 83*(4), Article 106386.
Makido, Y., Dhakal, S., & Yamagata, Y. (2012). Relationship between urban form and CO_2 emissions: Evidence from fifty Japanese cities[J]. *Urban Climate, 2*, 55–67.
Mubarek, S., Koomen, E., Estreguil, C., et al. (2011). Development of a composite index of urban compactness for land use modelling applications[J]. *Landscape and Urban Planning, 103*(3–4), 303–317.
Oda, T., Maksyutov, S., & Andres, R. J. (2018). The open-source data inventory for anthropogenic carbon dioxide (CO_2), version 2016 (ODIAC2016): A global, monthly fossil-fuel CO_2 gridded emission data product for tracer transport simulations and surface flux inversions[J]. *Earth System Science Data, 10*, 87–107.
Qin, B., & Wu, J. (2015). Does urban concentration mitigate CO_2 emissions? Evidence from China 1998–2008[J]. *China Economic Review, 35*, 220–231.
Ramaswami, A., Jiang, D., Tong, K., et al. (2018). Impact of the economic structure of cities on urban scaling factors: Implications for urban material and energy flows in China[J]. *Journal of Industrial Ecology, 22*(2), 392–405.
Shi, K., Huang, C., Yu, B., et al. (2014). Evaluation of NPP-VIIRS night-time light composite data for extracting built-up urban areas[J]. *Remote Sensing Letters, 5*(4), 358–366.
Shi, K., Li, Y., Chen, Y., et al. (2019). How does the urban form $PM_{2.5}$ concentration relationship change seasonally in Chinese cities? A comparative analysis between national and urban agglomeration scales[J]. *Journal of Cleaner Production, 239*, 118088.1–118088.13.
Shi, K., Shen, J., Wu, Y., et al. (2021). Carbon dioxide (CO_2) emissions from the service industry, traffic, and secondary industry as revealed by the remotely sensed nighttime light data[J]. *International Journal of Digital Earth*, 1–14.
Shi, K., Wang, H., Yang, Q., et al. (2019). Exploring the relationships between urban forms and fine particulate ($PM_{2.5}$) concentration in China: A multi-perspective study [J]. *Journal of Cleaner Production, 231*, 990–1004.
Shi, K., Yu, B., Huang, Y., et al. (2014). Evaluating the ability of NPP-VIIRS nighttime light data to estimate the gross domestic product and the electric power consumption of China at multiple scales: A comparison with DMSP-OLS data[J]. *Remote Sensing, 6*(2), 1705–1724.
Sperling, J. B., & Ramaswami, A. (2013). Exploring health outcomes as a motivator for low-carbon city development: Implications for infrastructure interventions in Asian cities[J]. *Habitat International, 37*(1), 113–123.
State Council. (2014). *Notice on adjusting the standard of city size division*.
Sun, B., Han, S., & Li, W. (2020). Effects of the polycentric spatial structures of Chinese city regions on CO_2 concentrations[J]. *Transportation Research Part D Transport and Environment, 82*(2), Article 102333.
Tang, L., & Cui, H. (2017). Improvement of urban construction land extraction method based on NPP-VIIRS nighttime light data and Landsat-8 data: A case study of Guangzhou City[J]. *Geomatics&Spatial Information Technology, 40*(9), 69–73 (in Chinese).
Wang, S., & Huang, Y. (2019). Spatial spillover effect and driving forces of carbon emission intensity at city level in China[J]. *Acta Geographica Sinica, 74*(6), 1131–1148 (in Chinese).
Wang, S., Wang, J., Fang, C., et al. (2019a). Estimating the impacts of urban form on CO_2 emission efficiency in the Pearl River Delta, China[J]. *Cities, 85*, 117–129.
Wang, S., Wang, J., Fang, C., et al. (2019b). Estimating the impacts of urban form on CO_2 emission efficiency in the Pearl River Delta, China[J]. *Cities, 85*, 117–129.
Wang, Y., & Wang, J. (2019). Does industrial agglomeration facilitate environmental performance: New evidence from urban China?[J]. *Journal of Environmental Management, 248*, Article 109244.
Wilson, B. (2013). Urban form and residential electricity consumption: Evidence from Illinois, USA[J]. *Landscape and Urban Planning, 115*, 62–71.
Xie, Y., Weng, Q., & Fu, P. (2019). Temporal variations of artificial nighttime lights and their implications for urbanization in the conterminous United States, 2013–2017 [J]. *Remote Sensing of Environment, 225*, 160–174.
Yang, W., Li, T., & Cao, X. (2015). Examining the impacts of socio-economic factors, urban form and transportation development on CO2 emissions from transportation in China: a panel data analysis of China's provinces[J]. *Habitat International, 49*, 212–220.
Yang, Y., Wu, J., Wang, Y., et al. (2021). Quantifying spatiotemporal patterns of shrinking cities in urbanizing China: A novel approach based on time-series nighttime light data[J]. *Cities, 118*, Article 103346.
Yao, X., Kou, D., Shao, S., et al. (2018). Can urbanization process and carbon emission abatement be harmonious? New evidence from China[J]. *Environmental Impact Assessment Review, 71*, 70–83.
Ye, C., Zhu, J., Li, S., et al. (2018). Assessment and analysis of regional economic collaborative development within an urban agglomeration: Yangtze River Delta as a case study[J]. *Habitat International, 83*, 20–29.
Zhao, F. A., Jian, P. B., & Jwa, B. (2022). Using DMSP/OLS nighttime light data and K–means method to identify urban–rural fringe of megacities[J]. *Habitat International, 103*, 102227.
Zhao, H., Cao, X., & Ma, T. (2020). A spatial econometric empirical research on the impact of industrial agglomeration on haze pollution in China[J]. *Air Quality, Atmosphere and Health, 13*(11), 1305–1312.
Zhao, J., Dong, X., & Dong, K. (2021). How does producer services' agglomeration promote carbon reduction?: The case of China[J]. *Economic Modelling, 104*, Article 105624.
Zhao, M., Zhou, Y., Li, X., et al. (2020). Mapping urban dynamics (1992–2018) in Southeast Asia using consistent nighttime light data from DMSP and VIIRS[J]. *Remote Sensing of Environment, 248*, Article 111980.
Zhou, Y., Li, C., Zheng, W., et al. (2021). Identification of urban shrinkage using NPP-VIIRS nighttime light data at the county level in China[J]. *Cities, 118*, Article 103373.
Zhou, Y., Smith, S. J., Elvidge, C. D., et al. (2014). A cluster-based method to map urban area from DMSP/OLS nightlights[J]. *Remote Sensing of Environment, 147*, 173–185.